A T-Matrix Theory of Galactic Heavy-Ion Fragmentation

John W. Norbury,
Lawrence W. Townsend,
and Philip A. Deutchman

NASA
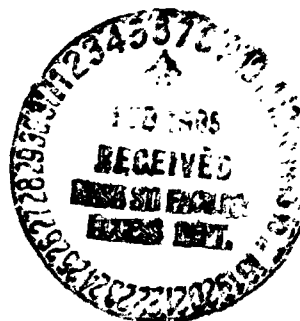
NASA
Technical
Paper
2363

1985

A T-Matrix Theory of Galactic Heavy-Ion Fragmentation

John W. Norbury
Old Dominion University
Norfolk, Virginia

Lawrence W. Townsend
Langley Research Center
Hampton, Virginia

Philip A. Deutchman
University of Idaho
Moscow, Idaho

Summary

The theory of galactic heavy-ion fragmentation has been furthered by incorporating a T-matrix approach into the description of the three-step process of abrasion, ablation, and final-state interactions. The connection between this T-matrix and the interaction potential is derived. The resulting transition rate is shown to be independent of the choice of the initial time. For resonant states, the substitution of complex energies for real energies is formally justified for up to third-order processes.

The previously developed abrasion-ablation fragmentation theory is rederived from first principles and is shown to result from time-ordering, classical-probability, and zero-width resonance approximations. Improvements in the accuracy of the total fragmentation cross sections would require an alternative to the latter two approximations. Since a more rigorous test of the theory would be to compare theoretical and experimental differential cross sections, a Lorentz-invariant differential abrasion-ablation cross section is derived which explicitly includes the previously derived abrasion total cross sections. This result requires the use of the time-ordering and classical probability assumptions. It is demonstrated that spectral and angular distributions could be easily obtained from the general Lorentz-invariant form. Future success in calculating these distributions will require the evaluation of the ablation T-matrix, which is the remaining formidable task.

Introduction

Research efforts are currently under way to develop methods for protecting astronauts from the potentially harmful effects of cosmic rays. These effects are particularly important for astronauts on long-duration missions and for career space workers making repeated journeys into space in the era of the Space Station and the Space Transportation System, because a biologically significant component of cosmic rays consists of relativistic nuclei (ref. 1). Theories are presently being developed to accurately describe their interactions with matter (refs. 2 through 6). In previous work, an optical model potential approximation to the exact nucleus-nucleus multiple scattering series has been used, within the context of eikonal scattering theory (refs. 3 and 4), to accurately predict total abrasion cross sections. This method has been extended (ref. 6) to calculate isotopic and elemental total fragmentation cross sections by essentially multiplying the total abrasion cross section by the following two factors: (1) a charge dispersion fraction giving the probability that z of the abraded nucleons are protons, and (2) a compound nucleus decay probability which describes the de-excitation (ablation) of an excited projectile nucleus prefragment. Final-state interactions (ref. 7), which describe the interactions between the abraded nucleons and the remaining projectile prefragment, are not yet included in the theory.

Because of greater flexibility in comparing theory with experiment, it is advantageous to develop methods for calculating Lorentz-invariant differential cross sections. Aside from direct comparisons with experimental data, angular and spectral distributions are easily obtained for any reference frame (e.g., nucleus-nucleus center of mass, nucleon-nucleon center of mass, laboratory, etc.). Angular distributions obtained from eikonal theory are usually evaluated in the laboratory frame, and transformations to another reference frame are laborious (ref. 8). In addition, eikonal theory is not readily generalized to calculate the Lorentz-invariant differential cross sections which are often used to present experimental data. Rather than simply multiplying the abrasion cross section by approximate factors to obtain ablation effects, it is desired to include ablation in a more fundamental and exact manner by explicitly calculating ablation matrix elements.

With the preceding considerations in mind, a first-principles derivation of the transition rate is presented herein. The transition rate formally includes abrasion, ablation, and final-state interaction matrix elements and is easily generalized to produce Lorentz-invariant differential cross sections. The interaction potentials V and transition operators $\hat{T}$ introduced herein are used to describe the three-step process of abrasion, ablation, and final-state interaction. This generalization is the main conceptual difference between their use in references 2 and 3, where they were directly connected to an optical model description of abrasion only, and their use in the present work.

Evaluation of Amplitudes

The fundamental equations for the probability amplitudes are derived in this section. The full Hamiltonian H consists of an unperturbed piece H_o and an additional interaction V, such that

$$H = H_o + V \tag{1}$$

The eigenstates and eigen-energies of H_o are obtained from

$$H_o|n> = \epsilon_n|n> \tag{2}$$

The full wave function Ψ is determined from the time-dependent Schrödinger equation

$$H\Psi = i\hbar\frac{\partial\Psi}{\partial t} \tag{3}$$

This wave function is expanded in terms of the complete,

orthonormal set of unperturbed states $|n>$ generated by H_o as

$$\Psi = \sum_n c_n(t) \exp(-i\epsilon_n t/\hbar)|n> \qquad (4)$$

Substituting equation (4) into equation (3) yields (refs. 9 and 10)

$$\frac{dc_k(t)}{dt} = \frac{1}{i\hbar} \sum_n c_n(t) \exp(i\omega_{kn}t) V_{kn} \qquad (5)$$

which, for a time-independent interaction, has the solution

$$c_k(t) = \delta_{ki} + \frac{1}{i\hbar} \sum_n V_{kn} \int_{t_o}^{t} c_n(t') \exp(i\omega_{kn}t') dt' \qquad (6)$$

where

$$\omega_{kn} \equiv (\epsilon_k - \epsilon_n)/\hbar \qquad (7)$$

and

$$V_{kn} \equiv <k|V|n> \qquad (8)$$

Equation (5) is exact, is of fundamental importance, and does not require V_{kn} to be small, as might be assumed.

The weak incompletely coupled approximation (WICA) is defined as

$$\frac{dc_k(t)}{dt} \approx \frac{1}{i\hbar} c_i(t) \exp(i\omega_{ki}t) V_{ki} \qquad (9)$$

where

$$\omega_{ki} \equiv (\epsilon_k - \epsilon_i)/\hbar \qquad (10)$$

and

$$V_{ki} \equiv <k|V|i> \qquad (11)$$

with the initial, fully populated state at time t_o denoted by $|i>$. This approximation (eq. (9)) uncouples $c_k(t)$ from all other amplitudes except $c_i(t)$ and suggests that the regeneration or depletion of a particular state depends only upon its being fed from or decaying to one other state. As is discussed subsequently, this approximation is equivalent to neglecting higher-order terms in the interaction matrix elements.

The strong incompletely coupled approximation (SICA) sets

$$c_n(t) = \delta_{ni} \qquad (12)$$

in equation (5) to give

$$\frac{dc_k(t)}{dt} \approx \frac{1}{i\hbar} \exp(i\omega_{ki}t) V_{ki} \qquad (13)$$

This equation is valid only for times which are short compared with the lifetime of the initial state (i.e., $c_k(t) << c_i(t)$). If the perturbation V is transient and small in magnitude, the amplitudes $c_k(t)$ will remain small for all times. Thus, equation (13) is most commonly used for scattering problems with small perturbing interaction potentials. In contrast, the WICA (eq. (9)) is appropriate when studying a decaying state over a period of time equal to several half-lives. Therefore, the WICA is appropriate for evaluating resonance states, since their complex energy widths result in the usual exponential decay. The solutions of equations (9) and (13) are identical except for the appearance of complex energies in equation (9) where real energies are found in equation (13). Thus, one of the major results of the present work is the demonstration that real energies can be simply replaced by complex energies when studying resonances.

Real-Energy Transition Amplitude

In this section, equation (5) is integrated directly to yield an "exact" amplitude. A convergence factor, $\alpha \rightarrow 0^+$, will be inserted to render the integral convergent for a nonfinite initial time ($t_o \rightarrow -\infty$), where αt is much smaller than unity. Thus, equation (6) becomes

$$c_k(t) = \delta_{ki} + \frac{1}{i\hbar} \sum_n V_{kn}$$

$$\times \int_{t_o}^{t} c_n(t') \exp(i\omega_{kn}t' + \alpha t') dt' \qquad (14)$$

and analogously,

$$c_n(t') = \delta_{ni} + \frac{1}{i\hbar} \sum_l V_{li}$$

$$\times \int_{t_o}^{t'} c_l(t'') \exp(i\omega_{li}t'' + \alpha t'') dt'' \qquad (15)$$

In equations (14) and (15), the correct method is to take the limit as $\alpha \rightarrow 0^+$ after taking the limit as $t_o \rightarrow -\infty$. Also, the convergence factor α is not required (Set = 0 before performing the integrals) for a finite initial time (e.g., $t_o = 0$).

Inserting equation (15) into equation (14) and expanding yields and iterative result as follows:

$$c_k(t) = \delta_{ki} + \frac{1}{i\hbar} V_{kn} \int_{t_o}^{t} \exp\left(i\omega_{ki}t' + \alpha t'\right) dt'$$

$$+ \frac{1}{(i\hbar)^2} \sum_n V_{kn} V_{ni} \int_{t_o}^{t} \left[\int_{t_o}^{t'} \exp\left(i\omega_{ni}t''\right.\right.$$

$$\left.\left. + \alpha t''\right) dt'' \right] \exp\left(i\omega_{kn}t' + \alpha t'\right) dt'$$

$$+ \frac{1}{(i\hbar)^3} \sum_n \sum_l V_{kn} V_{nl} V_{li} \int_{t_o}^{t} \left\{ \int_{t_o}^{t'} \left[\int_{t_o}^{t''} \exp\left(i\omega_{li}t'''\right.\right.\right.$$

$$\left.\left.\left. + \alpha t'''\right) d_l{}''' \right] \exp\left(i\omega_{nl}t'' + \alpha t''\right) dt'' \right\}$$

$$\times \exp\left(i\omega_{kn}t' + \alpha t'\right) dt' + \ldots \tag{16}$$

Evaluating these integrals gives

$$c_k(t) = \delta_{ki} + \frac{1}{\hbar} V_{ki} \frac{\exp\left(i\omega_{ki}t + \alpha t\right) - \exp\left(i\omega_{ki}t_o + \alpha t_o\right)}{-\omega_{ki} + i\alpha}$$

$$+ \frac{1}{\hbar^2} \sum_n V_{kn} V_{ni} \left\{ \frac{\exp\left(i\omega_{ki}t + 2\alpha t\right) - \exp\left(i\omega_{ki}t_o + 2\alpha t_o\right)}{(-\omega_{ni} + i\alpha)(-\omega_{ki} + i\alpha)} \right.$$

$$\left. - \frac{\exp\left(i\omega_{ni}t_o + \alpha t_o\right)\left[\exp\left(i\omega_{kn}t + \alpha t\right) - \exp(i\omega_{kn}t_o + 2\alpha t_o)\right]}{(-\omega_{ni} + i\alpha)(-\omega_{kn} + i\alpha)} \right\}$$

$$+ \frac{1}{\hbar^3} \sum_n \sum_l V_{kn} V_{nl} V_{li}$$

$$\times \left\{ \frac{\exp\left(i\omega_{ki}t + 3\alpha t\right) - \exp\left(i\omega_{kn}t_o + 3\alpha t_o\right)}{(-\omega_{ki} + i3\alpha)(-\omega_{li} + i\alpha)(-\omega_{ni} + i2\alpha)} \right.$$

$$+ \frac{\exp\left(i\omega_{ni}t_o + 2\alpha t_o\right)\left[\exp\left(i\omega_{kn}t + \alpha t\right) - \exp(i\omega_{kn}t_o + \alpha t_o)\right]}{(-\omega_{kn} + i\alpha)(-\omega_{ni} + i\alpha)(-\omega_{nl} + i\alpha)}$$

$$\left. - \frac{\exp\left(i\omega_{ki}t_o + \alpha t_o\right)\left[\exp(i\omega_{ki}t + 2\alpha t) - \exp(i\omega_{ki}t_o + 2\alpha t_o)\right]}{(-\omega_{kl} + i2\alpha)(-\omega_{li} + i\alpha)(-\omega_{nl} + i\alpha)} \right\} + \ldots$$

$$\tag{17}$$

Equation (17) is the exact final-state amplitude derived from equation (14).

Real-Energy Perturbation Theory and the SICA

In this section, a much more compact form for the amplitude is derived through the introduction of a T-matrix. An ansatz suggested (ref. 10) by the SICA (eq. (13)) is written as

$$c_k(t) = \delta_{ki} + \frac{1}{i\hbar} T_{ki} \int_{t_o}^{t} \exp\left(i\omega_{ki}t' + \alpha t'\right) dt' \tag{18}$$

where the convergence factor is again inserted to render the integral convergent for nonfinite initial time $(t_o \rightarrow -\infty)$, and T_{ki} is a transition matrix element whose relationship to V_{ki} will be determined. Evaluating the integral in equation (18) and taking the limit as $t_o \rightarrow -\infty$ before taking the limit as $\alpha \rightarrow 0^+$ yields

$$c_k(t, t_o \rightarrow -\infty) = \delta_{ki} + \frac{T_{ki}}{\hbar(-\omega_{ki} + i\alpha)} \exp\left(i\omega_{ki}t + \alpha t\right) \tag{19}$$

For a finite value of t_o, the convergence factor is not required and equation (18) becomes

$$c_k(t, t_o) = \delta_{ki} + \frac{T_{ki}}{-\hbar\omega_{ki}} \exp(i\omega_{ki}t_o)\left\{\exp[i\omega_{ki}(t - t_o)] - 1\right\} \tag{20}$$

Substituting equation (18), and the analogous expression for $c_n(t, t_o \rightarrow -\infty)$, into equation (5) yields the relationship between T and V as

$$T_{ki} = V_{ki} + \sum_n \frac{V_{kn} T_{ni}}{\hbar(-\omega_{ni} + i\alpha)} \tag{21}$$

This same result (eq. (21)) can be obtained from the exact solution (eq. (17)) by taking the limit as $t_o \rightarrow -\infty$ in equation (17), substituting equation (19) into the left-hand side of equation (17), and solving for T_{ki}.

Identifying the denominator in equation (21) as the Green function G_{ni} and using a modified Einstein summation convention for triply repeated indices enables equation (21) to be written as

$$T_{ki} = V_{ki} + V_{kn} G_{ni} T_{ni} \tag{22}$$

or, in operator form, as

$$\hat{T} = V + VG\hat{T} \tag{23}$$

This is the usual result from scattering theory (ref. 10).

Because of its extreme compactness and simplicity, equation (19) would be useful for the fundamental amplitudes in applications to the heavy-ion fragmentation problem. There are, however, some questions concerning its general applicability: (1) how do the solutions depend upon the choice of the initial time t_o; and (2) how does one include a description of resonances, which require complex energies, rather than the real energies used previously. These questions are addressed in the following sections.

Transition Rates and the Initial Time

The choice of a nonfinite initial time ($t_o \to -\infty$) is appropriate in a scattering situation to ensure that possibly spurious transient terms are not introduced when the scattering region suddenly experiences the full potential at time t_o. It is, however, worthwhile to determine what effect the choice of t_o has on the experimentally measurable transition rate (or cross section).

Clearly, the amplitudes given by equations (19) and (20) differ for different values of t_o. The transition rate is defined as

$$w = \lim_{t \to \infty} \frac{dP(t)}{dt} \qquad (24)$$

where, for discrete final states, the probability is

$$P(t) = \sum_k P_k(t) \qquad (25)$$

and for continuous final states,

$$P(t) = \int \rho(\epsilon_k) P_k(t) \, d\epsilon_k \qquad (26)$$

with the probability related to the amplitude as

$$P_k(t) = |c_k(t)|^2 \qquad (27)$$

From equation (19),

$$\frac{d}{dt} |c_k(t, t_o \to -\infty)|^2 = \frac{2\alpha}{\hbar^2 \left(\omega_{ki}^2 + \alpha^2 \right)} \exp(2\alpha t) |T_{ki}|^2 \qquad (28)$$

which, upon taking the limit as $\alpha \to 0^+$, becomes

$$\lim_{\alpha \to 0^+} \frac{d}{dt} |c_k(t, t_o \to -\infty)|^2 = \frac{2\pi}{\hbar^2} \delta(\omega_{ki}) |T_{ki}|^2 \qquad (29)$$

Since the right-hand side of equation (29) does not change for the limit as $t \to \infty$, the transition rate becomes

$$w = \frac{2\pi}{\hbar} |T_{ki}|^2 \rho(\epsilon_k) \qquad (30)$$

Equation (30) is a fundamental result. In a similar manner, equation (20) yields

$$\frac{d}{dt} |c_k(t, t_o)|^2 = \frac{1}{\hbar^2} |T_{ki}|^2 \frac{2 \sin(\omega_{ki} t)}{\omega_{ki}} \qquad (31)$$

Equation (31) yields

$$\lim_{t \to \infty} \frac{d}{dt} |c_k(t, t_o)|^2 = \frac{2\pi}{\hbar^2} \delta(\omega_{ki}) |T_{ki}|^2 \qquad (32)$$

which is identical to equation (29). Hence, the transition rate is independent of the choice of the initial time.

Resonances and Complex Energies

In previous work (refs. 6 and 11), an abrasion-ablation model was developed to describe heavy-ion fragmentation. A possible source of disagreement between theoretical predictions and the available experimental data might be uncertainties in the excitation energies of the excited projectile prefragments (refs. 6 and 12). In reference 6 it was assumed that the prefragment could be treated as an excited compound nucleus. An alternative approach would be to use a nuclear cascade description (ref. 13). Since a correct description of the excited prefragment is essential in predicting fragmentation cross section, a description incorporating an intranuclear cascade followed by a compound nucleus evaporation process may be required.

The treatment of resonances, such as for the compound nucleus (ref. 14), requires the use of complex energies (ref. 9). In first-order theory, Merzbacher (ref. 10) has shown how to use complex energies to describe resonances, and Norbury and Deutchman (ref. 9) have shown the same thing in second-order theory. Both of these presentations, however, depend upon the use of the WICA (eq. (9)). As previously mentioned, the consideration of final-state interactions, together with abrasion-ablation, requires, in principle, third-order matrix elements. To accomplish this it is shown subsequently how to include complex energies beyond second order without the use of an incompletely coupled approximation.

The basic second-order process involves a transition from an initial state $|i\rangle$ to an intermediate resonating state $|n\rangle$, followed by subsequent decay to the final state $|k\rangle$. This transition involves the use of three coupled equations of the type given in equation (5), whereas Merzbacher (ref. 10) uses only two coupled equations to extract the first-order process. The rate of change of the

intermediate-state coefficients is given by

$$\frac{dc_n(t)}{dt} = \frac{1}{i\hbar} \sum_l c_l(t) \exp(i\omega_{nl}t) V_{nl} \qquad (33)$$

where the rates of change of the $c_l(t)$ are given by

$$\frac{dc_l(t)}{dt} = \frac{1}{i\hbar} \sum_m c_m(t) \exp(i\omega_{lm}t) V_{lm} \qquad (34)$$

In reference 9, Norbury and Deutchman solved these equations by assuming the WICA form for equation (34) as

$$\frac{dc_l(t)}{dt} = \frac{1}{i\hbar} c_m(t) \exp(i\omega_{lm}t) V_{lm} \qquad (35)$$

In the present work, the full equation (34) is considered. A key factor, however, in the solubility of the three coupled equations (eqs. (5), (33), and (34)) is the separation of equation (34) as

$$\frac{dc_l(t)}{dt} = \frac{1}{i\hbar} c_n(t) \exp(i\omega_{ln}t) V_{ln}$$

$$+ \frac{1}{i\hbar} \sum_{m \neq n} c_m(t) \exp(i\omega_{lm}t) V_{lm} \qquad (36)$$

so that the first term is simply the right-hand side of equation (35), which is the WICA contribution.

Integrating equation (36) yields

$$c_l(t) = \delta_{li} + \frac{V_{ln}}{i\hbar} \int_{t_o}^{t} c_n(t') \exp(i\omega_{ln}t') \, dt'$$

$$+ \frac{1}{i\hbar} \sum_{m \neq n} V_{lm} \int_{t_o}^{t} c_m(t') \exp(i\omega_{lm}t') \, dt' \qquad (37)$$

where

$$c_l(t_o) = \delta_{li} \qquad (38)$$

Equation (33) is rewritten as

$$\frac{dc_n(t)}{dt} = \frac{V_{nn}}{i\hbar} c_n(t) + \frac{1}{i\hbar} \sum_{l \neq n} c_l(t) \exp(i\omega_{nl}t) V_{nl} \qquad (39)$$

which, upon substitution of equation (37) becomes

$$\frac{dc_n(t)}{dt} = \frac{V_{ni}}{i\hbar} \exp(i\omega_{ni}t) + \frac{V_{nn}}{i\hbar} c_n(t)$$

$$+ \frac{1}{(i\hbar)^2} \sum_{l \neq n} |V_{nl}|^2 \exp(i\omega_{nl}t) \int_{t_o}^{t} c_n(t') \exp(i\omega_{ln}t') \, dt'$$

$$+ \frac{1}{(i\hbar)^2} \sum_{l \neq n} \sum_{m \neq n} V_{nl} V_{lm} \exp(i\omega_{nl}t)$$

$$\times \int_{t_o}^{t} c_m(t') \exp(i\omega_{lm}t') \, dt' \qquad (40)$$

Because of the substitution of the Kronecker delta term from equation (37) into the summation term in equation (39), $n \neq i$ in V_{ni}. Because $l \neq n$ in equation (39) the δ_{li} in equation (37) implies that $n \neq i$ in V_{ni}.

The solution of equation (40) $c_n(t)$ appears complicated but can be simplified by reducing equation (40) to an algebraic expression through the use of a Fourier transform pair, defined as

$$c_n(t) \equiv \int_{-\infty}^{\infty} f_n(\omega) \exp(-i\omega t) \, d\omega \qquad (41)$$

and

$$f_n(\omega) \equiv \frac{1}{2\pi} \int_{-\infty}^{\infty} c_n(t) \exp(i\omega t) \, dt \qquad (42)$$

Assuming

$$c_n(t \leq t_o) = 0 \qquad (43)$$

for the intermediate state, equation (42) becomes

$$f_n(\omega) = \frac{1}{2\pi} \int_{t_o}^{\infty} c_n(t) \exp(i\omega t) \, dt \qquad (44)$$

Multiplying equation (40) by $\exp[i(\omega + i\alpha)t]$ and integrating from t_o to ∞ yields

$$\int_{t_o}^{\infty} \exp\left[i(\omega + i\alpha)t\right]\frac{dc_n(t)}{dt}\,dt$$

$$= \frac{V_{ni}}{i\hbar} \int_{t_o}^{\infty} \exp\left[i(\omega_{ni} + \omega + i\alpha)t\right]\,dt$$

$$+ \frac{V_{nn}}{i\hbar} \int_{t_o}^{\infty} c_n(t)\exp\left[i(\omega + i\alpha)t\right]\,dt$$

$$+ \frac{1}{(i\hbar)^2} \sum_{l\neq n} \left|V_{ln}\right|^2 \int_{t_o}^{\infty} \exp\left[i(\omega_{nl} + \omega + i\alpha)t\right]$$

$$\times \left[\int_{t_o}^{t} c_n(t')\exp\left(i\omega_{ln}t'\right)\,dt'\right]dt$$

$$+ \frac{1}{(i\hbar)^2} \sum_{l\neq n}\sum_{m\neq n} V_{nl}V_{lm}$$

$$\times \int_{t_o}^{\infty} \exp\left[i(\omega_{nl} + \omega + i\alpha)t\right]$$

$$\times \left[\int_{t_o}^{t} c_m(t')\exp\left(i\omega_{lm}t'\right)\,dt'\right]dt \qquad (45)$$

where the α factors have been inserted to render the integrals convergent. Upon evaluation of these integrals, equation (45) becomes

$$-2\pi i\,(\omega + i\alpha)\,f_n(\omega)$$

$$= \frac{V_{ni}}{\hbar}\,\frac{\exp\left[i(\omega_{ni} + \omega + i\alpha)t_o\right]}{\omega_{ni} + \omega + i\alpha}$$

$$+ \frac{V_{nn}}{i\hbar}\,2\pi\,f_n(\omega)$$

$$- \frac{2\pi}{(i\hbar)^2} \sum_{l\neq n} \left|V_{ln}\right|^2 \frac{f_n(\omega)}{i(\omega_{nl} + \omega) - \alpha}$$

$$- \frac{1}{(i\hbar)^2} \sum_{l\neq n}\sum_{m\neq n} \frac{V_{nl}V_{lm}}{i(\omega + \omega_{nl}) - \alpha}$$

$$\times \int_{t_o}^{\infty} \exp\left[i(\omega_{nm} + \omega + i\alpha)t'\right]\,c_m(t')\,dt' \qquad (46)$$

Solving for $f_n(\omega)$ and taking the inverse Fourier transform yields

$$2\pi i \int_{-\infty}^{\infty} f_n(\omega)\exp\left(-i\omega t\right)\,d\omega$$

$$= \frac{V_{ni}}{\hbar} \exp\left[i(\omega_{ni} + i\alpha)t_o\right]$$

$$\times \int_{-\infty}^{\infty} \frac{\exp\left[i\omega(t_o - t)\right]\,d\omega}{(\omega + \omega_{ni} + i\alpha)\left[-(\omega + i\alpha) + \xi(\omega)\right]}$$

$$+ \frac{1}{\hbar^2} \sum_{l\neq n}\sum_{m\neq n} V_{nl}V_{lm}$$

$$\times \int_{-\infty}^{\infty} \frac{\left\{\int_{t_o}^{\infty} \exp\left[i(\omega + \omega_{nm} + i\alpha)t'\right]\,c_m(t')\,dt'\right\}\exp\left(-i\omega t\right)\,d\omega}{\left[i(\omega_{nl} + \omega) - \alpha\right]\left[-(\omega + i\alpha) + \xi(\omega)\right]}$$

$$\tag{47}$$

with

$$\xi(\omega) = \frac{V_{nn}}{\hbar} + \frac{1}{\hbar^2} \sum_{l\neq n} \frac{\left|V_{ln}\right|^2}{\omega_{nl} + \omega + i\alpha} \qquad (48)$$

Evaluation of the integrals in equation (47) is simplified by assuming (ref. 10) that

$$\xi(\omega) \approx \xi(0) \qquad (49)$$

and inserting Dirac's identity (ref. 15)

$$\lim_{\alpha \to 0^+} \xi(0) = \frac{\Delta\epsilon_n}{\hbar} - \frac{i}{\hbar}\frac{\Gamma}{2} \qquad (50)$$

6

where the energy shift $\Delta\epsilon_n$ and the width Γ are defined as

$$\Delta\epsilon_n \equiv V_{nn} + \sum_{l \neq n} \frac{|V_{nl}|^2}{\epsilon_n - \epsilon_l} \qquad (51)$$

and

$$\frac{\Gamma}{2} \equiv \pi \sum_{l \neq n} |V_{nl}|^2 \, \delta(\epsilon_n - \epsilon_l) \qquad (52)$$

The left-hand side of equation (47) is just $2\pi i\, c_n(t)$. Using equations (51) and (52), equation (47) is rewritten as

$$2\pi i\, c_n(t) = \frac{V_{ni}}{\hbar} \exp\left[i(\omega_{ni} + i\alpha)t_o\right] I_0(t)$$

$$+ \frac{1}{\hbar^2} \sum_{l \neq n} \sum_{m \neq n} V_{nl}\, V_{lm}\, I(t) \qquad (53)$$

where

$$I_0(t) \equiv \int_{-\infty}^{\infty} \frac{\exp\left[i\omega(t_o - t)\right] d\omega}{(\omega + \omega_{ni} + i\alpha)\left(-\omega + \frac{\Delta\epsilon_n}{\hbar} - \frac{i}{\hbar}\frac{\Gamma'}{2} - i\alpha\right)} \qquad (54)$$

and

$$I(t) = \int_{-\infty}^{\infty} \frac{\left\{\int_{t_o}^{\infty} \exp[i(\omega + \omega_{nm} + i\alpha)t']\, c_m(t')\, dt'\right\} \exp(-i\omega t)\, d\omega}{[i(\omega_{ni} + \omega) - \alpha]\left(-\omega + \frac{\Delta\epsilon_n}{\hbar} - \frac{i}{\hbar}\frac{\Gamma}{2} - i\alpha\right)} \qquad (55)$$

Equation (54) has two simple poles at

$$\omega_1 = -(\omega_{ni} + i\alpha) \qquad (56)$$

and

$$\omega_2 = \frac{\Delta\epsilon_n}{\hbar} - \frac{i}{\hbar}\frac{\Gamma}{2} - i\alpha \qquad (57)$$

For $t < t_o$, a contour taken in the upper half plane of figure 1 gives

$$I_0(t < t_o) = 0 \qquad (58)$$

since no poles are enclosed. For $I_0(t > t_o)$, the lower contour, which encloses the poles, is used to yield

$$I_0(t > t_o) = \frac{-2\pi i\hbar}{\Delta\epsilon_n - \frac{i\Gamma}{2} + \epsilon_n - \epsilon_i}$$

$$\times \left\{ \exp\left[i(\omega_{ni} + i\alpha)\,(t - t_o)\right] \right.$$

$$\left. - \exp\left[-i(\Delta\epsilon_n - i\Gamma/2 - i\alpha\hbar)(t - t_o)/\hbar\right]\right\} \qquad (59)$$

The complex energy $\tilde{\epsilon}_n$ for the intermediate state $|n>$ is now defined as

$$\tilde{\epsilon}_n \equiv \epsilon_n + \Delta\epsilon_n - i\Gamma/2 \qquad (60)$$

Equation (47) then becomes

$$c_n(t > t_o) = \frac{V_{ni} \exp(i\omega_{ni}t)}{\epsilon_i - \tilde{\epsilon}_n}$$

$$\times \left\{1 - \exp\left[i(\epsilon_i - \tilde{\epsilon}_n)(t - t_o)/\hbar\right]\right\}$$

$$+ \frac{1}{2\pi i\hbar^2} \sum_{l \neq n} \sum_{m \neq n} V_{nl}\, V_{lm}\, I(t) \qquad (61)$$

Equation (61) is the probability amplitude for the intermediate resonating state. Note that $I(t)$ comes entirely from the second term on the right-hand side of equation (36). Thus, the first term on the right-hand side of equation (61) is the WICA contribution, and the second term is the contribution from higher order processes.

As a check of the preceding results (eq. (61)). set $I(t) = 0$ and consider the matching of initial conditions in the WICA. With $I(t) = 0$, equation (53) becomes

$$c_n(t) = \frac{V_{ni}}{2\pi i\hbar} \exp\left[i(\omega_{ni} + i\alpha)t_o\right] I_0(t) \qquad (62)$$

7

which, for $t < t_o$, yields

$$c_n(t < t_o) = 0 \qquad (63)$$

since $I_0(t < t_o) = 0$ from equation (58). From equation (61), for $t = t_o$,

$$c_n(t_o) = \frac{V_{ni}}{2\pi i \hbar} \exp \left[i(\omega_{ni} + i\alpha)t_o \right] I_0(t_o) = 0 \qquad (64)$$

since

$$I_0(t_o) = \int_{-\infty}^{\infty} \frac{d\omega}{(\omega - \omega_1)(-\omega + \omega_2)} = 0 \qquad (65)$$

using standard contour integration techniques. Thus, equations (63) and (64) satisfy the initial condition specified in equation (43). For $t > t_o$ and $I(t) = 0$, equation (61) becomes

$$c_n(t > t_o) = \frac{V_{ni} \exp(i\omega_{ni}t)}{\epsilon_i - \tilde{\epsilon}_n}$$

$$\times \left\{ 1 - \exp \left[i(\epsilon_i - \tilde{\epsilon}_n)(t - t_o)/\hbar \right] \right\} \qquad (66)$$

The derivative of equation (66) is

$$\frac{dc_n(t > t_o)}{dt} = \frac{V_{ni} \exp(i\omega_{ni}t)}{\epsilon_i - \tilde{\epsilon}_n}$$

$$\times \frac{i}{\hbar} \left\{ (\epsilon_n - \epsilon_i) - (\epsilon_n - \tilde{\epsilon}_n) \right.$$

$$\times \exp \left[i(\epsilon_i - \tilde{\epsilon}_n)(t - t_o)/\hbar \right] \right\} \qquad (67)$$

which, yields in the limit as $t \to t_o$,

$$\frac{dc_n(t_o)}{dt} = \frac{V_{ni} \exp(i\omega_{ni}t_o)}{i\hbar} \qquad (68)$$

This expression satisfies equation (33) when equation (37) is substituted (after letting $t \to t_o$). Thus, the initial conditions are satisfied in the WICA.

The final-state amplitude is evaluated here by rewriting equation (5) as follows:

$$\frac{dc_k(t)}{dt} = \frac{1}{i\hbar} c_i(t) \exp(i\omega_{ki}t) V_{ki}$$

$$+ \frac{1}{i\hbar} \sum_{n \neq i} c_n(t) \exp(i\omega_{kn}t) V_{kn} \qquad (69)$$

where $c_n(t)$ is given by equation (61). Our interest lies in processes which proceed via the formation and decay of intermediate states. Thus, we will ignore the term involving V_{ki}, since it will be negligible or zero. Therefore, substituting equation (61) into equation (69) and integrating from t_o to t yields

$$c_k(t) = \sum_{n \neq i} \frac{V_{kn} V_{ki}}{\tilde{\epsilon}_n - \epsilon_i} \exp(i\omega_{ki}t_o)$$

$$\times \left\{ \frac{\exp \left[i\omega_{ki}(t - t_o) \right] - 1}{\epsilon_k - \epsilon_i} \right.$$

$$\left. - \frac{\exp \left[i(\epsilon_k - \tilde{\epsilon}_n)(t - t_o)/\hbar \right] - 1}{\epsilon_k - \tilde{\epsilon}_n} \right\}$$

$$- \frac{1}{2\pi \hbar^3} \sum_{n} \sum_{l \neq n} \sum_{m \neq n} V_{kn} V_{nl} V_{lm}$$

$$\times \int_{t_o}^{t} \exp(i\omega_{kn}t'') I(t'') dt'' \qquad (70)$$

Equation (70) shows that the WICA is equivalent to neglecting at least third-order terms compared with second-order terms in the final-state amplitude.

As was done previously for the intermediate-state amplitude, the final-state amplitude within the WICA is evaluated for the initial conditions, which are

$$c_k(t \leq t_o) = 0 \qquad (71)$$

and

$$\frac{dc_k(t_o)}{dt} = 0 \qquad (72)$$

8

In equation (71), it is assumed that, before turning on the interaction at t_o, the system is in its initial state. Equation (72) is obtained from equation (5), with the initial condition on the intermediate state specified by equation (43) inserted. For $t = t_o$, equation (70) satisfies equation (71) trivially. Differentiating equation (70) and setting $t = t_o$ then satisfies equation (72).

Finally, the integral $I(t)$ is evaluated. Solution of equation (55) requires knowledge of $c_m(t')$. Using only the lowest-order contribution

$$c_m(t') = \delta_{mi} \tag{73}$$

yields

$$I(t) = \int_{-\infty}^{\infty} \frac{\left\{ \int_{t_o}^{\infty} \exp\left[i(\omega + \omega_{ni} + i\alpha)t'\right] dt' \right\} \exp(-i\omega t)\, d\omega}{[i(\omega + \omega_{ni}) - \alpha]\left(-\omega + \dfrac{\Delta\epsilon_n}{\hbar} - \dfrac{i}{\hbar}\dfrac{\Gamma}{2} - i\alpha\right)} \tag{74}$$

Evaluating equation (74) using the same contour integration techniques used previously to solve $I_o(t)$ enable the final-state amplitude from equation (70) to be written as

$$c_k(t) = \sum_{n \neq i} \frac{V_{kn} V_{ni}}{\tilde{\epsilon}_n - \epsilon_i} \exp(i\omega_{ki}t_o)\left\{ \frac{\exp[i\omega_{ki}(t - t_o)] - 1}{\epsilon_k - \epsilon_i} \right.$$

$$\left. - \frac{\exp[i(\tilde{\epsilon}_k - \epsilon_n)(t - t_o)/\hbar] - 1}{\epsilon_k - \tilde{\epsilon}_n} \right\}$$

$$- \sum_n \sum_{l \neq n, i} V_{kn} V_{nl} V_{li} \exp(i\omega_{ki}t_o)$$

$$\times \left\{ \frac{\exp[i\omega_{ki}(t - t_o)] - 1}{(\epsilon_k - \epsilon_i)(\epsilon_i - \epsilon_l)(\epsilon_i - \tilde{\epsilon}_n)} \right.$$

$$- \frac{\exp[i\omega_{kl}(t - t_o)] - 1}{(\epsilon_k - \epsilon_l)(\epsilon_i - \epsilon_l)(\epsilon_l - \tilde{\epsilon}_n)}$$

$$\left. + \frac{\exp[i(\epsilon_k - \tilde{\epsilon}_n)(t - t_o)/\hbar] - 1}{(\epsilon_k - \tilde{\epsilon}_n)(\epsilon_i - \tilde{\epsilon}_n)(\epsilon_l - \tilde{\epsilon}_n)} \right\}$$

$$+ \ldots \tag{75}$$

If the result for $\alpha = 0$ in equation (17) is compared with equation (75), the second-order and higher terms are identical if the real energies ϵ_n in equation (17) are replaced by complex energies $\tilde{\epsilon}_n$. These results, taken with the similar results of references 9 and 10, demonstrate that it is permissible to replace real energies with complex energies, of the form given by equation (60), when studying resonances.

Evaluation of Abrasion-Ablation T-Matrix

The basic Feynman diagram for projectile fragmentation, with fireball formation, is shown in figure 2. The diagram is similar to those presented elsewhere (refs. 16 through 18). Since our major interest is in the area of projectile fragmentation, target fragmentation and the formation and de-excitation of the fireball are not discussed in this paper.

Recently, there has been considerable interest in relativistic coulomb dissociation and the excitation of nuclear giant resonances (refs. 19 through 25). The typical method for describing these excitations is through the interaction of the projectile with an equivalent target phonon. The excitation process is then described in a manner analogous to a photonuclear reaction. The basic Feynman diagram for coulomb dissociation is given in reference 20. The excitation of a giant resonance may be important in determining projectile prefragment charge dispersions (ref. 12) and requires further study. Since our primary interest is in projectile fragmentation, this process, rather than fireball formation, is emphasized in the Feynman diagram. If the fragmentation process is thought of as a collection of A projectile nucleons suddenly being excited into a prefragment, then by analogy with coulomb dissociation, the excitation process can be treated as the interaction between a phonon field and the initial A nucleons in the projectile. The Feynman diagram for this phonon excitation process is shown in figure 3. Since the fireball is difficult to depict, it is simply represented as two separate projectile and target pieces. Figure 3 is only an alternative, and more convenient, way of depicting the interaction shown in figure 2, and the diagrams yield identical results. In the actual fragmentation process shown in figure 2, there is no direct interaction between the target and excited prefragment.

To simplify the phase space, the separate phase spaces of the individual particles can be replaced by a single phase-space factor describing the center of mass of those particles. Therefore, the fireball and target fragment are replaced here by target recoil T' and projectile recoil R pieces, since we are not interested in the details of the phase spaces of these pieces. This Feynman diagram, which is used in this analysis, is shown in figure 4. The projectile recoil piece R is not the projectile prefragment P'. Figure 4 is exactly analogous to a 4-body final-state

Feynman diagram (fig. 5) used to describe pion production via isobar formation and decay (refs. 9, 16, and 26 through 30). This Feynman diagram has recently been replaced (refs. 16 and 31) by the 3-body diagram (fig. 6), in which the pion escapes but the nucleon is recaptured by the projectile nucleus.

When developing expressions for the T-matrices, attention is focused on the interactions occurring in the projectile prefragment. (See fig. 7.) As noted in the following section, the prefragment interactions in figures 4 and 7 represent only the lowest-order interaction. Higher-order terms are subsequently discussed in detail.

The Two-Potential Problem

In the basic fragmentation process it is assumed that the projectile nucleus experiences an interaction V^1 and undergoes abrasion. (See fig. 7.) The projectile prefragment then experiences a different potential V^2 and ablates to yield the final fragment. This type of "two-potential" problem is considered in references 32 through 34, and the simplest solution is stated in the pion-production work of Townsend et al. (ref. 30).

The T-matrix expansion for abrasion-ablation (AA) is

$$T^{AA}_{ki} = V_{ki} + V_{kn}G_{nl}V_{ni}$$

$$+ V_{kn}G_{ni}V_{nm}G_{mi}V_{mi} + \dots \tag{76}$$

where an Einstein summation convention on triply repeated indices is implied. The full interaction potential is separated into abrasion V^1 and ablation V^2 pieces as

$$V = V^1 + V^2 \tag{77}$$

Inserting equation (77) into equation (76) and expanding yields

$$\begin{aligned}
T^{AA}_{ki} = {}& V^1_{ki} + V^2_{ki} + V^1_{kn}G_{ni}V^1_{ni} \\
& + V^2_{kn}G_{ni}V^1_{ni} + V^1_{kn}G_{ni}V^2_{ni} + V^2_{kn}G_{ni}V^2_{ni} \\
& + V^1_{kn}G_{ni}V^1_{nm}G_{mi}V^1_{mi} + V^1_{kn}G_{ni}V^1_{nm}G_{mi}V^2_{mi} \\
& + V^1_{kn}G_{ni}V^2_{nm}G_{mi}V^1_{mi} + V^1_{kn}G_{ni}V^2_{nm}G_{mi}V^2_{mi} \\
& + V^2_{kn}G_{ni}V^1_{nm}G_{mi}V^1_{mi} + V^2_{kn}G_{ni}V^1_{nm}G_{mi}V^2_{mi} \\
& + V^2_{kn}G_{ni}V^2_{nm}G_{mi}V^1_{mi} + V^2_{kn}G_{ni}V^2_{nm}G_{mi}V^2_{mi} \\
& + \dots \tag{78}
\end{aligned}$$

Each of these terms represents the higher-order generalizations of the Feynman diagram in figure 7. The Feynman diagrams, for the terms up to third order in equation (78), are shown in figures 8 through 11, where the abrasion V^1 is represented by a wavy line (phonon) and the ablation V^2 is represented by a heavy solid line. As discussed subsequently, the Feynman diagrams permit the abrasion-ablation process to proceed in a time-reversed fashion with the ablation occurring prior to the abrasion. Also, these diagrams do not include exchange terms (ref. 35), because such exchange diagrams yield negligible contributions.

Although equation (78) and its accompanying Feynman diagrams are quite complicated, they are shown only to third order and thus are not yet accurate enough for the present application. Ideally, interactions to infinite order should be included. This was effectively done for the abrasion step through the use of an eikonal scattering amplitude derived from an equivalent 1-body Schrödinger equation (refs. 2 and 4). This scattering amplitude is simply and directly related to the abrasion T-matrix which, by definition, includes abrasion interactions to infinite order. Since the T-matrix in equation (78) includes both abrasion and ablation, the full abrasion T-matrix must be extracted to incorporate the previously developed abrasion formalism (ref. 4). In other words, the abrasion potentials, to infinite order, must be factored out in equation (78).

The technique for factoring out the full abrasion T-matrix is most clearly seen by again considering the Feynman diagrams. In figure 11, the abrasion process to all orders is depicted along with their corresponding mathematical expressions. The simplest approach abrasion-ablation model would be to incorporate first-order ablation into the infinite-order abrasion formalism. (See fig. 12.) This is done by simply adding ablation bubbles to the abrasion diagrams in figure 11. Mathematically, this is equivalent to simply multiplying the abrasion series by $V^2_{kn}G_{ni}$ to yield

$$V^2_{kn}G_{ni}V^1_{ni} + V^2_{kn}G_{ni}V^1_{nm}G_{mi}V^1_{mi}$$

$$+ V^2_{kn}G_{ni}V^1_{nl}G_{li}V^1_{lm}G_{mi}V^1_{mi} + \dots$$

$$= V^2_{kn}G_{ni}\left(V^1_{ni} + V^1_{nm}G_{mi}V^1_{mi}\right.$$

$$\left. + V^1_{nl}G_{li}V^1_{lm}G_{mi}V^1_{mi} + \dots\right)$$

$$= V^2_{kn}G_{ni}T^{abr}_{ni} \tag{79}$$

so that the factorization of the abrasion T-matrix is apparent. In figure 13, second-order ablation coupled with infinite-order abrasion is presented. The corresponding series is then of the form

10

$$\left(V_{kl}^2 \, G_{li} \, V_{ln}^2 + V_{kn}^2 \right) \, G_{ni} \, T_{ni}^{abr}$$

$$+ \text{(time-reversal terms)} \tag{80}$$

where the time-reversal terms correspond to ablation occurring prior to abrasion. If these and any subsequent time-reversal terms from higher-order diagrams are ignored, the generalization to infinite-order abrasion-ablation clearly yields

$$T_{kl}^{AA} = \sum_n T_{kn}^{abl} \, G_{ni} \, T_{ni}^{abr} \tag{81}$$

This remarkable and extremely useful result arises entirely from equation (77) and the neglect of time-reversal Feynman diagrams. The neglect of these diagrams is henceforth dubbed as the "time-ordering approximation." Pilkᵘhn (eq. (3.15) of ref. 34) obtains a similar result when considering the time ordering of the time evolution operators (eq. (3.7) of ref. 34). For the purpose of this paper, equation (81) makes possible the incorporation of the infinite-order ablation processes into the previously developed infinite-order abrasion formalism (refs. 2 and 4).

Phase Space

In this section the definitions and recurrence relations for the Lorentz-invariant, noninvariant, and "normal" density-of-states factors are developed.

Lorentz-invariant phase space is given by the restricted phase-space element (refs. 34 and 36)

$$d \, \text{Lips} \, (\epsilon; p_1, p_2, \ldots, p_N)$$

$$= (2\pi)^4 \, \delta^4 \left(p - \sum_i p_i \right) \frac{1}{(2\pi)^{3N}} \prod_{i=1}^N \frac{d^3 p_i}{2\epsilon_i} \tag{82}$$

where the 4-body recurrence relation, in terms of 2-body phase spaces, is

$$d \, \text{Lips} \, (\epsilon; p_1, p_2, p_3, p_4) = \frac{1}{(2\pi)^2} \, d \, \text{Lips} \, (\epsilon; p_c, p_d)$$

$$\times \, d \, \text{Lips} \, (\epsilon_d; p_1, p_2)$$

$$\times \, d \, \text{Lips} \, (\epsilon_c; p_3, p_4) \, d \epsilon_c \, d \epsilon_d \tag{83}$$

where $d\epsilon_c$ and $d\epsilon_d$ represent integrations over the "nonobserved" particles.

The noninvariant phase space, which differs slightly from that given on page 388 of reference 33, is defined as

$$d \, \text{Nips} \, (\epsilon; p_1, p_2, \ldots, p_N) = \left[\frac{\nu}{(2\pi\hbar)^3} \right]^{N-1} \delta \left(\epsilon - \sum_i \epsilon_i \right)$$

$$\times \, \delta^3 \left(\vec{p} - \sum_i \vec{p_i} \right) \prod_{i=1}^N d^3 p_i \tag{84}$$

where ν is the normalization volume. For example, the corresponding recurrence relation for a 3-body phase space is given as

$$d \, \text{Nips} \, (\epsilon; p_1, p_2, p_3)$$

$$= d \, \text{Nips} \, (\epsilon; p_c, p_3)$$

$$\times \, d \, \text{Nips} \, (\epsilon_c, p_1, p_2) \, d\epsilon_c \tag{85}$$

Performing the momentum integrals over d Nips yields the usual density-of-states definition (ref. 37)

$$\rho, (\epsilon_k) = \int d \, \text{Nips} \, (\epsilon_k; p_1, p_2, \ldots, p_N)$$

$$= \left[\frac{\nu}{(2\pi\hbar)^3} \right]^{N-1} \int\!\!\int \ldots \int_{N-1}$$

$$\times \, d^3 p_1 \, d^3 p_2 \ldots d^3 p_{N-1} \, \delta \left(\epsilon_k - \sum_i \epsilon_i \right)$$

$$= \left[\frac{\nu}{(2\pi\hbar)^3} \right]^{N-1} \frac{d}{d\epsilon_k} \int\!\!\int \cdots \int_{N-1}$$

$$\times \, d^3 p_1 \, d^3 p_2 \ldots d^3 p_{N-1} \tag{86}$$

where ϵ_k is the sum of the final energies of the N particles. The recurrence relation for the N-body density of states is (ref. 16)

$$\rho_n(\epsilon_{12\ldots N}) = \int \cdots \int \rho_2(\epsilon_{12\cdots N}) \, \rho_2(\epsilon_{12\cdots N-1})$$

$$\times \, \rho_2(\epsilon_{12\ldots N-2}) \ldots \rho_2(\epsilon_{12}) \, d\epsilon_{12} \, d\epsilon_{123} \cdots d\epsilon_{12\cdots N-1} \tag{87}$$

where, for example,

$$\epsilon_{12\ldots N} \equiv \epsilon_1 + \epsilon_2 + \ldots + \epsilon_N \tag{88}$$

Abrasion-Ablation Model Derivation

In previous work (refs. 6 and 38), abrasion-ablation cross sections have been determined by calculating abrasion cross sections (refs. 3 and 4) which are then multiplied by an ablation probability obtained froᴧ compound nucleus decay probabilities (refs. 6 and 38). It is demonstrated in this section that this method of determining abrasion-ablation cross sections arises solely from particular approximations to the general formalism

developed herein, and is therefore only a special case of this more general formalism.

In terms of the transition rate, the total cross section is written as

$$\sigma = \frac{v}{v} w \qquad (89)$$

where v is the incident velocity of the projectile. Inserting equations (30) and (86) into equation (89), the total abrasion-ablation cross section for the phase space associated with figure 4 is

$$\sigma(Z) = \frac{2\pi v}{\hbar v} \frac{v^3}{(2\pi\hbar)^9} \frac{d}{d\epsilon_{ZXRT'}}$$

$$\times \iiint \left| T^{AA}_{kl} \right|^2 d^3 p_X \, d^3 p_{T'} \, d^3 p_Z \qquad (90)$$

Using a recurrence relation (ref. 16) derived from equation (86)

$$\rho_4(\epsilon_{ZXRT}) = \iiint \rho_2(\epsilon_{ZXRT})$$

$$\times \rho_2(\epsilon_{ZXR}) \rho_2(\epsilon_{ZX}) \, d\epsilon_{ZX} \, d\epsilon_{ZXR} \qquad (91)$$

demonstrates that $d^3 p_X$ can be replaced by $d^3 p_{P'}$ in equation (90) where

$$d^3 p_{P'} \equiv d^3 p_{ZX} \qquad (92)$$

This, together with equation (81), allows the cross section in equation (90) to be written as

$$\sigma(Z) = \frac{2\pi v}{\hbar v} \frac{v^3}{(2\pi\hbar)^9} \frac{d}{d\epsilon_{ZXRT'}} \iiint \left| \sum_n T^{abl}_{kn} G_{nl} T^{abr}_{rl} \right|^2$$

$$\times d^3 p_P \, d^3 p_{T'} \, d^3 p_Z \qquad (93)$$

A major approximation is now introduced as

$$\left| \sum_n T^{abl}_{kn} G_{nl} T^{abr}_{nl} \right|^2 \approx \sum_n \left| T^{abl}_{kn} \right|^2 \left| G_{nl} \right|^2 \left| T^{abr}_{nl} \right|^2 \qquad (94)$$

which will henceforth be referred to as the "classical probability approximation," since it involves the classical addition of probabilities (right-hand side) rather than the quantum mechanical addition of amplitudes (left-hand side). In essence, it involves ignoring the interference terms on the left-hand side of equation (94). It is our belief that the famous Bohr assumption for compound nucleus deca: (ref. 14), which justifies the separation of a two-step cross section (such as compound nucleus formation and decay, or abrasion-ablation) into a product of formation and decay (partial width) cross sections, is based upon this classical probability approximation. The Bohr assumption is so widely used because of the

reasonableness of the classical argument. Equation (94) is sometimes justified quantum mechanically, especially when dealing with angular-momentum matrix elements (refs. 32 and 39) where theorems on Clebsch-Gordan coefficients are available (ref. 16, chapter 4). This is especially true, for example, for a single (one-level) resonant state involving several different angular-momentum projections M (ref. 39), where the summation over n simply becomes a summation over M for the single resonance state of a particular energy. This was also the case for the pion production work of references 26 through 31, where there was only the single intermediate isobar Δ resonance at a fixed energy but with various spin and isotopic spin projections. Norbury (ref. 16) has shown that equation (94) results from the spin-isospin Clebsch-Gordan algebra. Another example is the photonuclear excitation of a compound nucleus where the formation of a resonant state of a single energy, but with different spin projections (ref. 40), justifies the use of the Bohr assumption when calculating (γ, n) cross sections via compound nucleus formation and decay. In general, however, the preceding simplifications which justify the classical probability assumption do not hold for the abrasion-ablation process. For example, a particular final projectile fragment could result from the ablation of numerous different prefragments, each with a quite different excitation energy.

The partial width, which is simply a transition rate multiplied by Planck's constant, is

$$\Gamma_n = 2\pi \frac{v}{(2\pi\hbar)^3} \frac{d}{d\epsilon_{P'}} \int \left| T^{abl}_{kn} \right|^2 d^3 p_Z \qquad (95)$$

Substituting equations (94) and (95) into equation (93) yields

$$\sigma(Z) = \sum_n \frac{v}{\hbar v} \frac{v^2}{(2\pi\hbar)^6} \frac{d}{d\epsilon_{ZXRT'}} \iiint \Gamma_n \left| G_{nl} \right|^2 \left| T^{abr}_{nl} \right|^2$$

$$\times d^3 p_P \, d^3 p_{T'} \, d\epsilon_{P'} \qquad (96)$$

which can be rewritten as

$$\sigma(Z) = \sum_n \frac{v}{\hbar v} \iint \Gamma_n \left| G_{nl} \right|^2 \left| T^{abr}_{nl} \right|^2$$

$$\times d \, \text{Nips} \, (\epsilon_{P'RT'}; p_{P'}, p_{R'}, p_{T'}) \, d\epsilon_{P'} \qquad (97)$$

The abrasion cross section is

$$\sigma_n(A) = \frac{2\pi v}{\hbar v} \int \left| T^{abr}_{nl} \right|^2$$

$$\times d \, \text{Nips} \, (\epsilon_{P'RT'}; p_{P'}, p_R, p_{T'}) \qquad (98)$$

12

which yields

$$\sigma(Z) = \frac{1}{2\pi} \sum_n \int \Gamma_n |G_{ni}|^2 \sigma_n(A) \, d\epsilon_{P'} \qquad (99)$$

Inserting the Green's function, the abrasion-ablation cross section is

$$\sigma(Z) = \frac{1}{2\pi} \sum_n \int \frac{\Gamma_n}{(\epsilon_n - \epsilon_i)^2 + (\Gamma/2)^2} \sigma_n(A) \, d\epsilon_{P'} \qquad (100)$$

where the total Γ and partial widths are related by

$$\Gamma = \sum_n \Gamma_n \qquad (101)$$

To evaluate the integral in equation (100), the zero-width approximation (ref. 34)

$$\lim_{\Gamma \to 0} \frac{\Gamma/2\pi}{(\epsilon_n - \epsilon_i)^2 + (\Gamma/2)^2} = \delta(\epsilon_n - \epsilon_i) \qquad (102)$$

is introduced. Writing the energies explicitly as

$$\epsilon_n = \epsilon_{P'} + \epsilon_{T'} + \epsilon_R \qquad (103)$$

with an initial-state energy given by

$$\epsilon_i = \epsilon_P + \epsilon_T \qquad (104)$$

and the final-state energy as

$$\epsilon_k = \epsilon_X + \epsilon_Z + \epsilon_{T'} + \epsilon_R \qquad (105)$$

then conservation of energy

$$\epsilon_k = \epsilon_i \qquad (106)$$

yields

$$\epsilon_n - \epsilon_i = \epsilon_{P'} - (\epsilon_X + \epsilon_Z) \qquad (107)$$

Inserting equation (107) into equation (100) indicates a variable, intermediate, virtual resonance energy $\epsilon_{P'}$ centered about $\epsilon_X + \epsilon_Z$, which is integrated over. The nature of the delta function in equation (102), however, destroys this quantum mechanical feature of virtual energy in the integral. The zero-width approximation, then, can be considered as another classical approximation. Inserting equations (102) and (107) in equation (100) yields

$$\sigma(Z) = \sum_n (\Gamma_n/\Gamma) \sigma_n(A) \qquad (108)$$

If the branching ratio is defined as

$$g_n \equiv \Gamma_n/\Gamma \qquad (109)$$

and is recognized as the usual ablation probability factor (refs. 6 and 38), then

$$\sigma(Z) = \sum_n g_n \sigma_n(A) \qquad (110)$$

which is the standard abrasion-ablation cross-section result (refs. 6, 7, 38, 41, and 42).

This result (eq. (110)) can also be obtained from equation (100) by an alternative method. Since $\sigma_n(A)$ is obtained by integrating over all impact parameters, it is independent of $\epsilon_{P'}$. Taking it outside the integral enables equation (100) to be written as

$$\sigma(Z) = \frac{1}{2\pi} \sum_n \sigma_n(A) \int \frac{\Gamma_n}{(\epsilon_n - \epsilon_i)^2 + (\Gamma/2)^2} \, d\epsilon_{P'} \qquad (111)$$

Inserting

$$\frac{\Gamma}{\Gamma} = 1 \qquad (112)$$

inside the integral in equation (111) and substituting equation (109) yields

$$\sigma(Z) = \frac{1}{2\pi} \sum_n \sigma_n(A) \int g_n \frac{\Gamma}{(\epsilon_n - \epsilon_i)^2 + (\Gamma/2)^2} \, d\epsilon_{P'} \qquad (113)$$

If g_n is independent of $\epsilon_{P'}$ (which merely requires Γ_n and Γ to possess the same energy dependence), then it can be taken outside the integral to yield

$$\sigma(Z) = \frac{1}{2\pi} \sum_n g_n \sigma_n(A) \int \frac{\Gamma}{(\epsilon_n - \epsilon_i)^2 + (\Gamma/2)^2} \, d\epsilon_{P'} \qquad (114)$$

In principle, if the dependence of Γ on $\epsilon_{P'}$ is known, then the integral can be calculated numerically if not analytically. If the zero-width approximation is inserted from equation (102), equation (110) is again obtained.

Equation (110) is one of the central results of the present work. It represents a first-principles derivation of the usual abrasion-ablation cross section and results directly from: (1) the time-ordering approximation, (2) the classical probability approximation, and (3) the zero-width approximation. Clearly then, the most obvious improvements to the abrasion-ablation theory would be to remove these assumptions (the time-ordering approximation is the least important). The zero-width approximation is removed in the next section.

Lorentz-Invariant Differential Cross Section

For an arbitrary number N of particles in the final state, the total cross section is

$$\sigma = \frac{2\pi\nu}{\hbar\nu}\left[\frac{\nu}{(2\pi\hbar)^3}\right]^{N-1}\frac{d}{d\epsilon_k}\iint \cdots \int_{N-1}$$

$$\times \left|T_{ki}^{AA}\right|^2 d^3p_1\, d^3p_2 \ldots d^3p_{N-1} \qquad (115)$$

For a specific final particle or fragment Z the differential cross section is

$$\frac{d^3\sigma(Z)}{dP_Z^3} = \frac{2\pi\nu}{\hbar\nu}\left[\frac{\nu}{(2\pi\hbar)^3}\right]^{N-1}$$

$$\times \frac{d}{d\epsilon_k}\int \cdots \int_{Z-1}\int_{Z+1}\cdots \int_{N-1}\left|T_{ki}^{AA}\right|^2$$

$$\times d^3p_1 \ldots d^3p_{Z-1}\, d^3p_{Z+1} \ldots d^3p_{N-1}$$

$$(116)$$

This is formally cast into Lorentz-invariant form as

$$\frac{d^3\sigma(Z)}{c^3(dp^3/\epsilon)_Z} = \frac{\epsilon_Z}{c^3}\frac{2\pi\nu}{\hbar\nu}\left[\frac{\nu}{(2\pi\hbar)^3}\right]^{N-1}\frac{d}{d\epsilon_k}\int \cdots \int_{Z-1}$$

$$\times \int_{Z+1}\cdots \int_{N-1}\left|T_{ki}^{AA}\right|^2 d^3p_1 \cdots d^3p_{Z-1}$$

$$\times d^3p_{Z+1} \ldots d^3p_{N-1} \qquad (117)$$

The ϵ_Z which appears in equation (117) is cancelled by an ϵ_Z which appears when the interaction matrix elements are explicitly evaluated.

Using

$$d^3p = p^2\, dp\, d\Omega \qquad (118)$$

it follows that

$$\left(\frac{d^2\sigma}{dp\, d\Omega}\right)_{frame} = \left(\frac{p^2}{\epsilon}\right)_{frame}\frac{d^3\sigma}{dp^3/\epsilon} \qquad (119)$$

and

$$\left(\frac{d^2\sigma}{d\epsilon\, d\Omega}\right)_{frame} = \left(\frac{p}{c^2}\right)_{frame}\frac{d^3\sigma}{dp^3/\epsilon} \qquad (120)$$

where $(d^3\sigma/dp^3/\epsilon)$ is the Lorentz-invariant differential cross section obtained from equation (117). The notation "frame" in equations (119) and (120) denotes that the specified quantity is evaluated in the desired reference frame, which is completely arbitrary. The angular $(d\sigma/d\Omega)$ and spectral $(d\sigma/d\epsilon)$ distributions are then obtained from equation (120) by performing the appropriate energy or angle integrations in that particular specified frame.

For the abrasion-ablation Feynman diagram of figure 4, the Lorentz-invariant differential cross section is

$$\frac{d^3\sigma(Z)}{c^3(dp^3/\epsilon)_Z} = \frac{\epsilon_Z}{c^3}\frac{2\pi\nu}{\hbar\nu}\frac{\nu^3}{(2\pi\hbar)^9}\frac{d}{d\epsilon_{ZXRT'}}$$

$$\times \iint\left|\sum_n T_{kn}^{abl}G_{ni}T_{ni}^{abr}\right|^2 d^3p_{P'}\, d^3p_{T'}$$

$$(121)$$

Employing the classical probability approximation and introducing d Nips, equation (121) becomes

$$\frac{d^3\sigma(Z)}{c^3(dp^3/\epsilon)_Z} = \frac{\epsilon_Z}{c^3}\frac{2\pi\nu}{\hbar\nu}\frac{\nu}{(2\pi\hbar)^3}$$

$$\times \sum_n\int\left|T_{kn}^{abl}\right|^2\left|G_{ni}\right|^2\left|T_{ni}^{abr}\right|^2$$

$$\times d\text{ Nips }(\epsilon_{P'RT'};p_{P'},p_R,p_{T'}) \qquad (122)$$

which, upon inserting equation (98), becomes

$$\frac{d^3\sigma(Z)}{c^3(dp^3/\epsilon)_Z} = \frac{\epsilon_Z}{c^3}\frac{\nu}{(2\pi\hbar)^3}$$

$$\times \sum_n\left|T_{kn}^{abl}\right|^2\left|G_{ni}\right|^2\sigma_n(A) \qquad (123)$$

Inserting the Green's function yields

$$\frac{d^3\sigma(Z)}{c^3(dp^3/\epsilon)_Z} = \frac{\epsilon_Z}{c^3}\frac{\nu}{(2\pi\hbar)^3}$$

$$\times \sum_n\frac{\left|T_{kn}^{abl}\right|^2\sigma_n(A)}{(\epsilon_n - \epsilon_i)^2 + (\Gamma/2)^2} \qquad (124)$$

which demonstrates the need to evaluate the ablation (decay) matrix elements directly (when dealing with differential cross sections) rather than using partial widths (see eq. (110)), as was done with total cross sections.

Equation (124) is a major result of the present work, since it provides the framework for calculating angular, spectral, and Lorentz-invariant distributions for the abrasion-ablation process in terms of the previously developed abrasion cross-section formalism (ref. 4). Fragment angular and spectral distributions can be obtained from equations (124) and (120) by performing the appropriate integrals. Clearly, the comparison of these distributions with experiment is of major importance in determining the accuracy of the present abrasion-ablation theory. Although these comparisons have not yet been done, equation (124) provides the framework necessary to do them. The remaining major task is to evaluate the ablation matrix element T_{kn}^{abl}.

References

1. Todd, Paul: Unique Biological Aspects of Radiation Hazards - An Overview. *Adv. Space Res.*, vol. 3, no. 8, 1983, pp. 187–194.

2. Wilson, J. W.; and Townsend, L. W.: An Optical Model for Composite Nuclear Scattering. *Canadian J. Phys.*, vol. 59, no. 11, Nov. 1981, pp. 1569–1576.

3. Townsend, Lawrence W.: *Optical-Model Abrasion Cross Sections for High-Energy Heavy Ions.* NASA TP-1893, 1981.

4. Townsend, L. W.: Abrasion Cross Sections for ^{20}Ne Projectiles at 2.1 GeV/Nucleon. *Canadian J. Phys.*, vol. 61, no. 1, Jan. 1983, pp. 93–98.

5. Townsend, Lawrence W.; Wilson, John W.; and Bidasaria, Hari B.: *Heavy-Ion Total and Absorption Cross Sections Above 25 MeV/Nucleon.* NASA TP-2138, 1983.

6. Townsend, Lawrence W.: *Ablation Effects in Oxygen-Lead Fragmentation at 2.1 GeV/Nucleon.* NASA TM-85704, 1984.

7. Hufner, J.; Schafer, K.; and Schurmann, B.: Abrasion-Ablation in Reactions Between Relativistic Heavy Ions. *Phys. Rev.*, ser. C, vol. 12, no. 6, Dec. 1975, pp. 1888–1898.

8. Maier, William B., II: *Transformations From Barycentric to Laboratory Coordinates for Two- and Three-Body Scattering Events.* LA-3972, Los Alamos Scientific Laboratory, Univ. of California, Mar. 1968.

9. Norbury, J. W.; and Deutchman, P. A.: Resonance Formation and Decay: An Application of Second-Order, Time-Dependent Perturbation Theory. *American J. Phys.*, vol. 52, no. 1, Jan. 1984, pp. 17–19.

10. Merzbacher, Eugen: *Quantum Mechanics,* Second ed. John Wiley & Sons, Inc. c.1970.

11. Wilson J. W.: Multiple Scattering of Heavy Ions, Glauber Theory, and Optical Model. Phys. Lett., vol. B52, no. 2, Sept. 1974, pp. 149–152.

12. Norbury, J. W.; Townsend, L. W.; and Wilson, J. W.: Fragmentation of Relativistic ^{16}O Projectiles by ^{9}Be and ^{208}Pb Target Nuclei. *Bull. American Phys. Soc.*, vol. 29, no. 4, 1984, p. 687.

13. Cugnon, J.; Mizutani, T.; and Vandermeulen, J.: Equilibration in Relativistic Nuclear Collisions. A Monte Carlo Calculation. *Nucl. Phys.* A, vol. 352, no. 3, Feb. 9, 1981, pp. 505–534.

14. Blatt, John M.; and Weisskopf, Victor F.: *Theoretical Nuclear Physics.* Springer-Verlag, c.1979, pp. 311–457.

15. Wyld, H. W.: *Mathematical Methods for Physics.* W. A. Benjamin, Inc. 1976, pp. 475–506.

16. Norbury, John William: Pion Production in Relativistic Heavy Ion Collisions. Ph. D. Diss., Univ. of Idaho Graduate School, Nov. 1983.

17. Wong, Che Yin: Peripheral and Central Collisions at Around 30 MeV per Nucleon. *5th High Energy Heavy Ion Study,* LBL-12652 (Contract W-7405-ENG-48), Lawrence Berkeley Lab., Univ. of California, Oct. 1981, pp. 61–86.

18. Friedman, William A.: Heavy Ion Projectile Fragmentation: Reexamination. *Phys. Rev.*, ser. C, vol. 27, no. 2, Feb. 1983, pp. 569–577.

19. Pilkuhn, H.: Dissociation of Relativistic Nuclei in the Nuclear Coulomb Field. *Phys. Lett.*, ser. B, vol. 38, no. 3, Feb. 7, 1972 pp. 143–146.

20. Artru, X.; and Yodh, G. B.: Coulomb Dissociation of Relativistic Nuclei. *Phys. Lett.*, ser. B., vol. 40, no. 1, Jun. 12, 1972, pp. 43–45.

21. Faldt, G.; Pilkuhn, H.; and Schlaile, H. G.: Nucleus-Nucleus Collisions at Relativistic Energies. *Ann. Phys.*, vol. 82, no. 2, Feb. 1974, pp. 326–344.

22. Heckman, Harry H.; and Lindstrom, Peter J.: Coulomb Dissociation of Relativistic ^{12}C and ^{16}O Nuclei. *Phys. Rev. Lett.*, vol. 37, no. 1, July 5, 1976, pp. 56–59.

23. Morrissey, D. J.; Marsh, W. R.; Otto, R. J.; Loveland, W.; and Seaborg, G. T.: Target Residue Mass and Charge Distributions in Relativistic Heavy Ion Reactions. *Phys. Rev.*, ser. C, vol. 18, no. 3, Sept. 1978, pp. 1267–1274.

24. Doll, P.; Hendrie, D. L.; Mahoney, J.; Menchaca-Roca, A.; Scott, D. K.; Symons, T. J. M.; Van Bibber, K.; Viyogi, Y. P.; and Wieman, H.: Giant-Resonance Studies With High-Energy Heavy Ions. *Phys. Rev. Lett.*, vol. 42, no. 6, 1979, pp. 366–369.

25. Mercier, M. T.; Hill, J. C.; Wohn, F. K.; and Smith, A. R.: Electromagnetic Dissociation of ^{197}Au by Relativistic Heavy Ions. *Phys. Rev. Lett.*, vol. 52, no. 11, Mar. 12, 1984, pp. 898–901.

26. Townsend, L. W.; and Deutchman, P. A.: Isobar Giant Resonance Formation in Self-Conjugate Nuclei. *Nucl. Phys. A*, vol. 355, 1981, pp. 505–532.

27. Deutchman, P. A.; and Townsend, L. W.: Coherent Isobar Production in Peripheral Relativistic Heavy-Ion Collisions. *Phys. Rev. Lett.*, vol. 45, no. 20, Nov. 17, 1980, pp. 1622–1625.

28. Deutchman, P. A.; and Townsend, L. W.: Isobars and Isobaric Analog States. *Phys. Rev.*, ser. C, vol. 25, no. 2, Feb. 1982, pp. 1105–1107.

29. Deutchman, P. A.; Madigan, R. L.; Norbury, J. W.; and Townsend, L. W.: Pion Production Through Coherent Isobar Formation in Heavy-Ion Collisions. *Phys. Lett.*, ser. B, vol. 132, no. 1, 2, 3, Nov. 24, 1983, pp. 44–46.

30. Townsend, L. W.; Deutchman, P. A.; Madigan, R. L.; and Norbury, J. W.: Pion Production Via Isobar Giant Resonance Formation and Decay. *Nucl. Phys. A*, vol. 415, Mar. 19, 1984, pp. 520–529.

31. Norbury, J. W.; Deutchman, P. A.; and Townsend, L. W.: A Particle-Hole Formalism for Pion Production From Isobar Formation and Decay in Peripheral Heavy Ion Collisions. *Bull. American Phys. Soc.*, vol. 29, no. 4, Apr. 1984, p. 688.

32. Goldberger, Marvin L.; and Watson, Kenneth M.: *Collision Theory.* John Wiley & Sons, Inc., c.1964, pp. 424–509.

33. Joachain, Charles J.: *Quantum Collision Theory.* American Elsevier Pub. Co., Inc. c.1975, pp. 344–374.

34. Pilkuhn, Hartmut: *The Interactions of Hadrons.* John Wiley & Sons, Inc., c.1967, pp. 26-51.

35. Aitchison, Ian J. R.; and Hey, Anthony J. G.: *Gauge Theories in Particle Physics.* Adam Hilger Ltd., c.1982.

36. Pilkuhn, Harmut M.: *Relativistic Particle Physics.* Springer-Verlag, c.1979.

37. Frauenfelder, Hans; and Henley, Ernest M.: *Subatomic Physics.* Prentice-Hall, Inc., c. 1974.

38. Townsend, Lawrence W.; Wilson, John W.; Norbury, John W.; and Bidasaria, Hari B.: *An Abrasion-Ablation Model Description of Galactic Heavy-Ion Fragmentation.* NASA TP-2305, 1984.

39. Brink, D.M.; and Satchler, G. R.: *Angular Momentum,* Second ed. Clarendon Press, 1968.

40. Norbury, J. W.; Thompson, M. N.; Shoda, K.; and Tsubota, H.: Photoneutron Cross Section of ^{54}Fe. *Australian J. Phys.*, vol. 31, no. 6, Dec. 1978, pp. 471–475.

41. Bowman, J. D.; Swiatecki, W. J.; and Tsang, C. F.: *Abrasion and Ablation of Heavy Ions.* LBL-2908, Univ. of California, July 1973.

42. Bleszynski, M.; and Sander, C.: Geometrical Aspects of High-Energy Peripheral Nucleus-Nucleus Collisions. *Nucl. Phys. A*, vol. 326, nos. 2-3, Sept. 10, 1979, pp. 525–535.

Symbols

A	mass number of final projectile prefragment
AA	abrasion-ablation process
c	speed of light, 3×10^8 m/sec
$c_i(t)$	initial-state probability amplitude
$c_k(t)$	final-state probability amplitude
$c_j(t)$	arbitrary-state probability amplitude
$c_n(t)$	intermediate-state probability amplitude
d Lips	Lorentz-invariant phase-space element
d Nips	Noninvariant phase-space element, MeV^{-1}
$d^3\sigma$	differential cross-section element, mb
$d\epsilon$	energy element, MeV
d^3p	momentum phase-space element, $(MeV/c)^3$
$d\Omega$	element of solid angle, sr
F'	highly excited fireball
$f_n(\omega)$	Fourier transform of probability amplitude
G	Green's operator, MeV^{-1}
G_{nt}	Green's function, MeV^{-1}
g_n	branching ratio
H	full Hamiltonian, MeV
H_o	unperturbed Hamiltonian, MeV
$\hbar$	Planck's constant $(6.58 \times 10^{-22}$ MeV-sec$)$
$I(t)$	time-dependent integral
$|i>$	initial-state vector
$|k>$	final-state vector
M	angular momentum projection, $MeV\text{-}fm\text{-}c^{-1}$
N	number of bodies in final state
$|n>$	intermediate-state vector
P	projectile
$P(t)$	total transition probability
$P_k(t)$	single-state transition probability
P'	excited prefragment
p	momentum, $MeV\text{-}c^{-1}$
R	recoil projectile
T	target
$\hat{T}$	transition operator, MeV
T_{kn}	transition matrix element, MeV
T'	recoil target
t	time, sec
t_o	initial time, sec
V	interaction potential, MeV
V_{kn}	matrix element of interaction potential, MeV
V^1	abrasion potential, MeV
V^2	ablation potential, MeV
v	incident projectile velocity, m/sec
w	transition rate, sec^{-1}
X	ablated projectile particles
Z	final projectile fragment
z	number of abraded protons
α	convergence factor
Γ	total decay width, MeV
Γ_n	partial decay width, MeV
γ	photon
Δ	intermediate isobar resonance

$\Delta\epsilon_n$	energy shift, MeV		

$\Delta\epsilon_n$ energy shift, MeV

δ_{ki} Kronecker delta

$\delta(\omega_{ki})$ Dirac delta function on frequency, sec

ϵ energy, MeV

ϵ_i initial-state energy, MeV

ϵ_k final-state energy, MeV

ϵ_n intermediate-state energy, MeV

ϵ_Z final energy of ablated particles, MeV

$\tilde{\epsilon}_n$ intermediate complex energy, MeV

ν volume normalization element, fm^3

$\rho(\epsilon_k)$ density of final states, MeV^{-1}

σ cross section, mb

Ψ full wave function

Ω solid angle, sr

ω angular frequency, sec^{-1}

ω_{kn} frequency difference between states $|k>$ and $|n>$, sec^{-1}

Subscripts:

i initial state

k final state

l arbitrary state

m arbitrary state

n intermediate state

P projectile

T target

Superscripts:

AA abrasion-ablation

abl ablation

abr abrasion
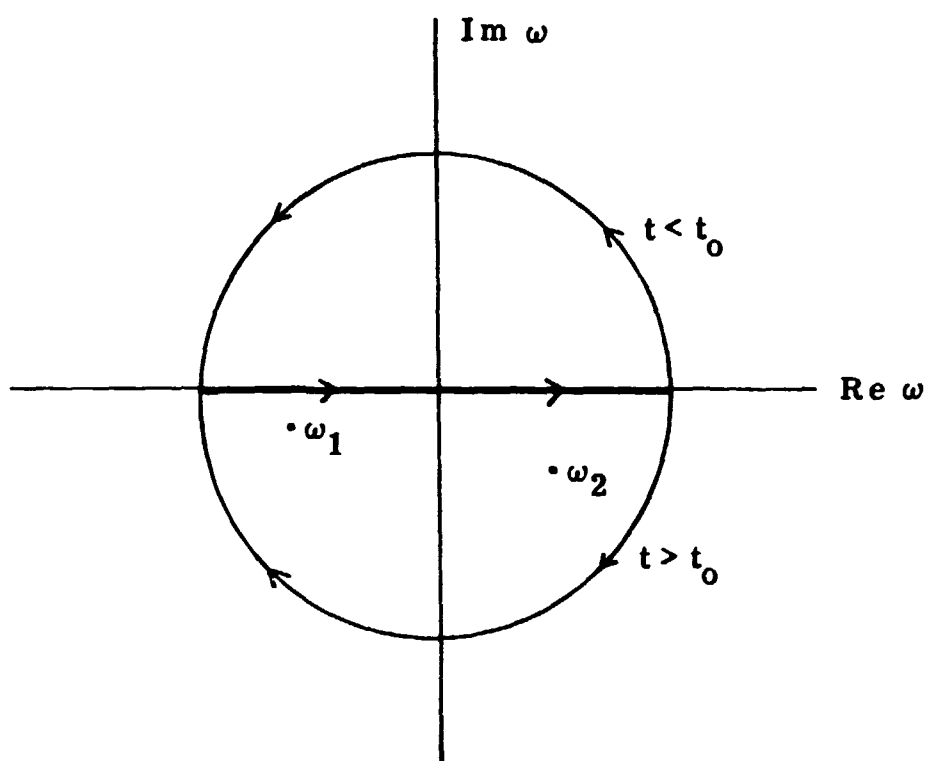
Figure 1. Contour for $I_o(t)$.
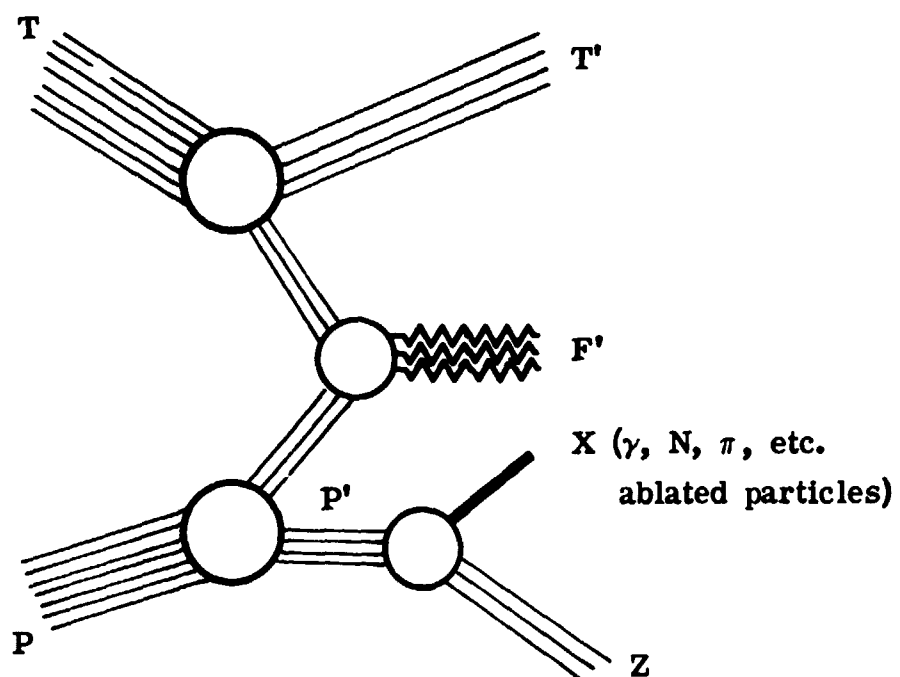
Figure 2. Feynman diagram of projectile fragmentation and fireball formation. (Final-state interactions are ignored.)
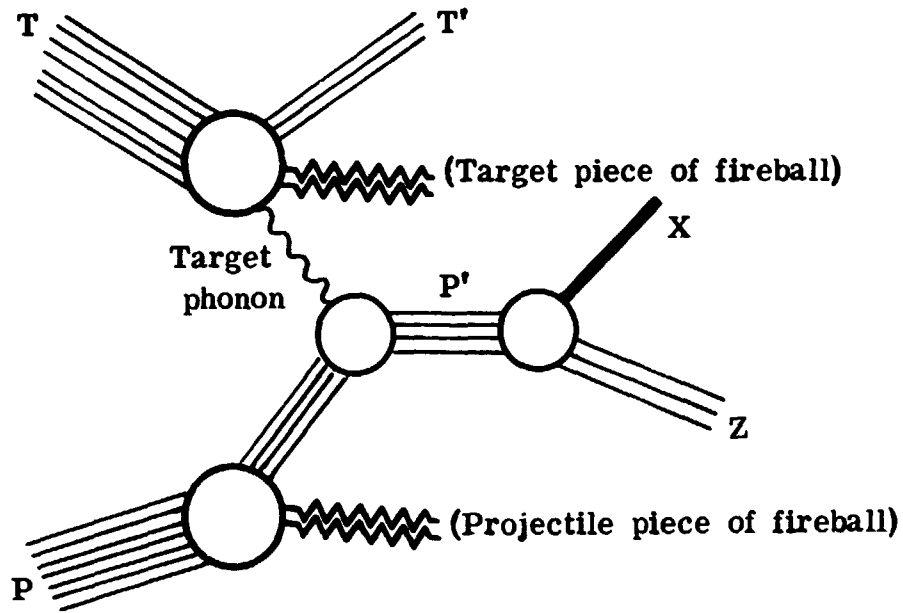
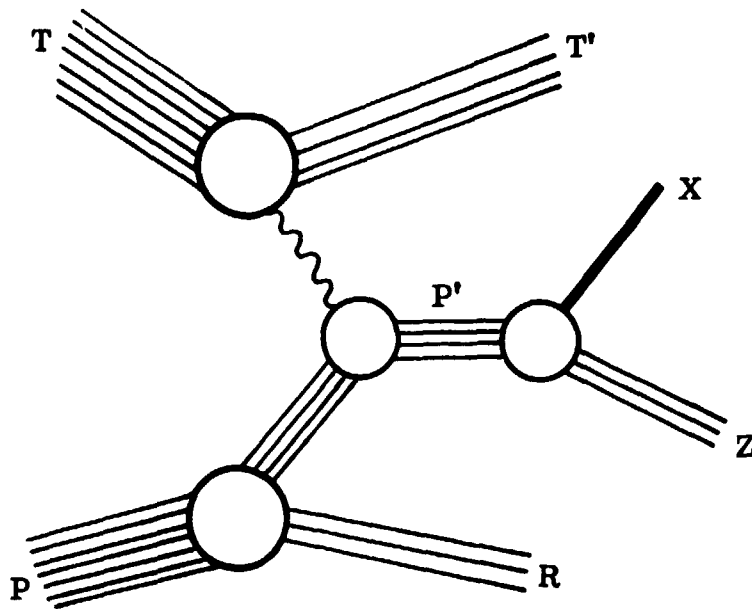Figure 3. Feynman diagram of equivalent target phonon excitation of projectile prefragment.

Figure 4. Equivalent Feynman diagram (lowest order; no time reversal) of projectile prefragmentation used in this work.
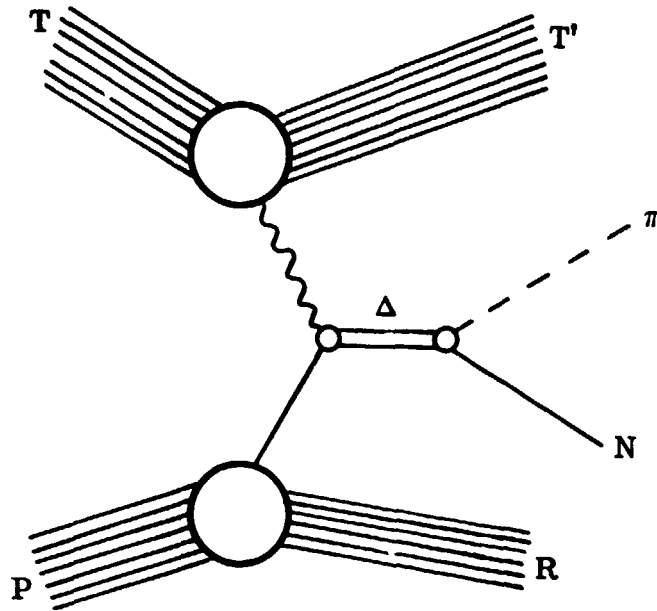
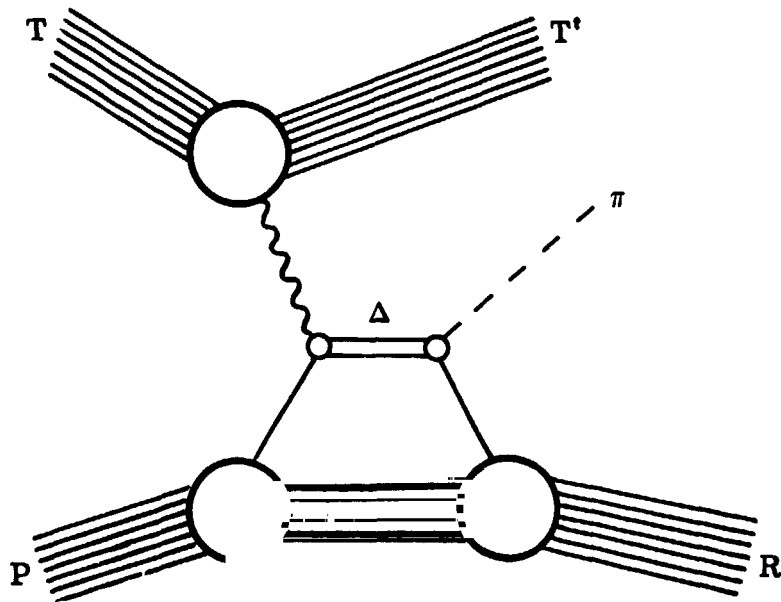Figure 5. Feynman diagram of pion production with 4-body final phase space.

Figure 6. Feynman diagram of pion production with 3-body final phase space.
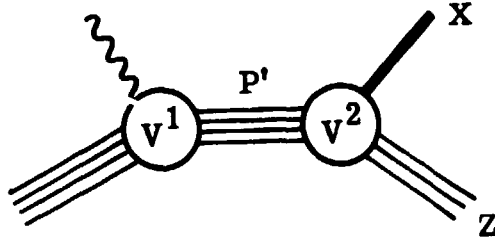
Figure 7. Lowest-order projectile prefrag-
ment interactions. Wavy line represents
abrasion V^1, and heavy solid line
represents ablation V^2.
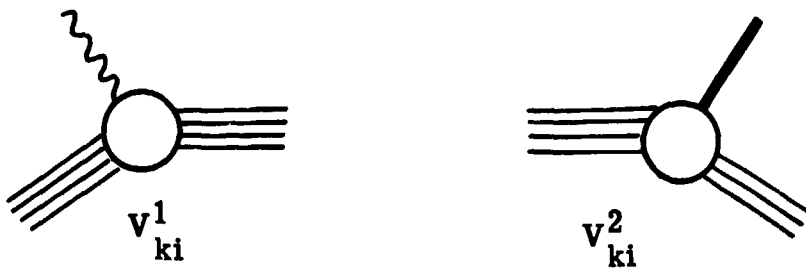
Figure 8. First-order matrix elements of abrasion-ablation T-matrix
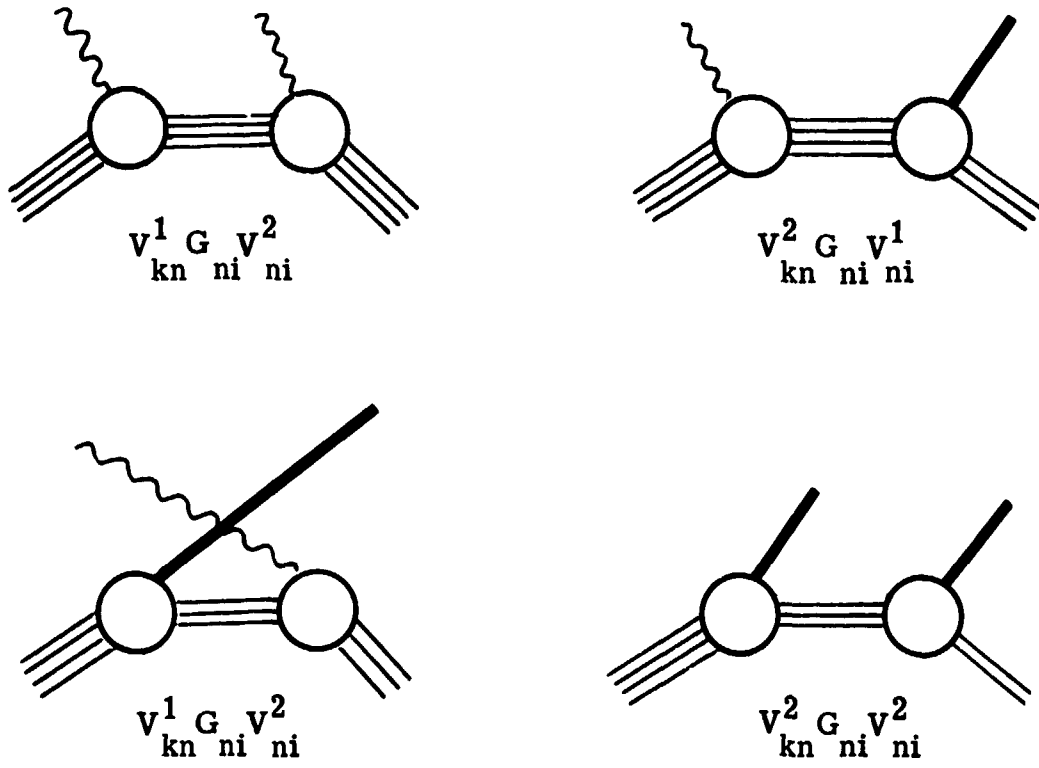in equation (78).

Figure 9. Second-order matrix elements of abrasion-ablation T-matrix in equation (78). (The first abrasion process on left-hand bubbles is that of figure 4. All other abrasion processes are only indicated schematically. Particle number conservation is not shown explicitly as it is for ablation.)
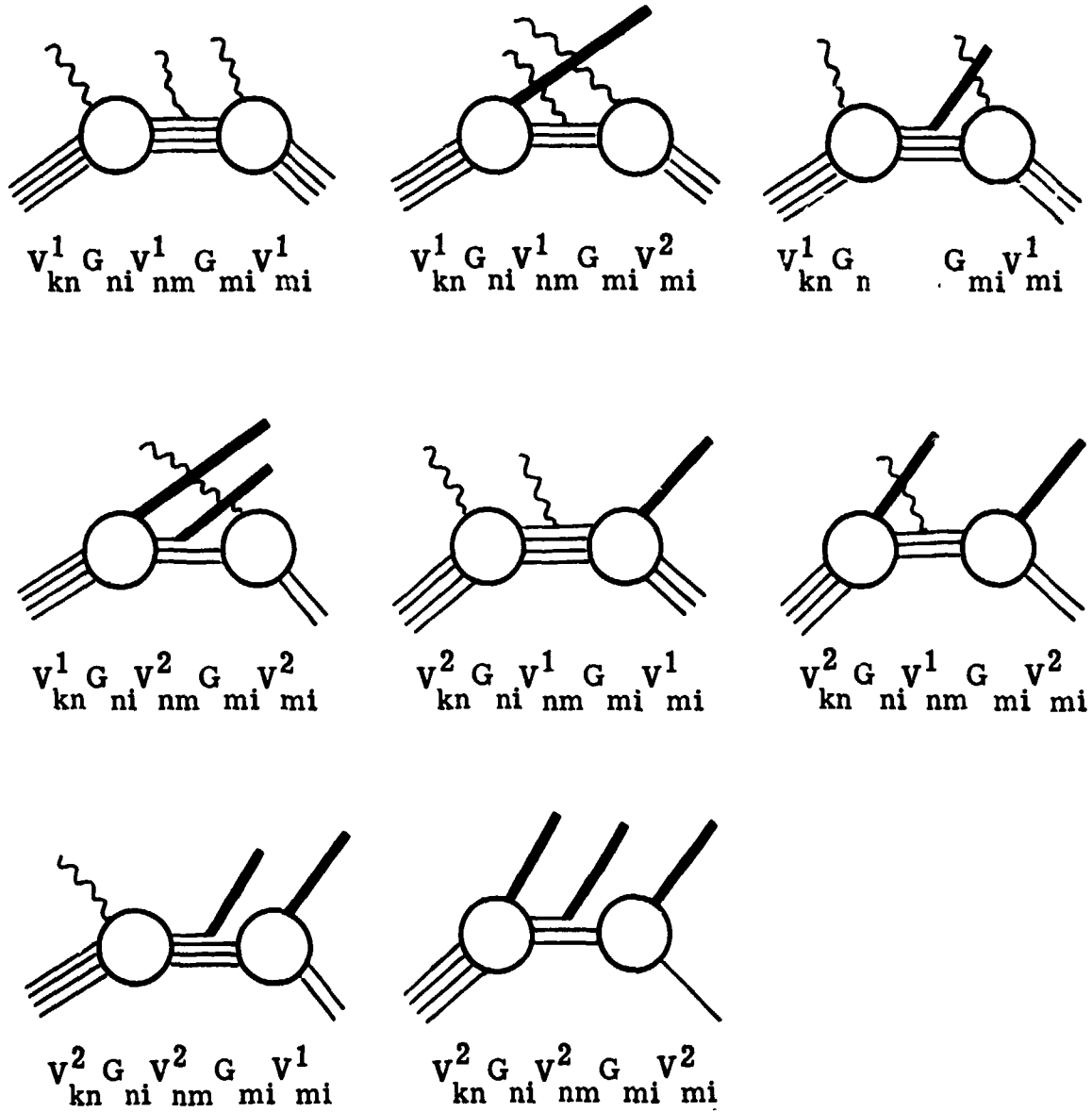
$$v^1_{kn} G_{ni} v^1_{nm} G_{mi} v^1_{mi} \qquad v^1_{kn} G_{ni} v^1_{nm} G_{mi} v^2_{mi} \qquad v^1_{kn} G_n \quad G_{mi} v^1_{mi}$$

$$v^1_{kn} G_{ni} v^2_{nm} G_{mi} v^2_{mi} \qquad v^2_{kn} G_{ni} v^1_{nm} G_{mi} v^1_{mi} \qquad v^2_{kn} G_{ni} v^1_{nm} G_{mi} v^2_{mi}$$

$$v^2_{kn} G_{ni} v^2_{nm} G_{mi} v^1_{mi} \qquad v^2_{kn} G_{ni} v^2_{nm} G_{mi} v^2_{mi}$$

Figure 10. Third-order matrix elements of abrasion-ablation T-matrix in equation (78). (Abrasions are indicated schematically as in fig. 9.)
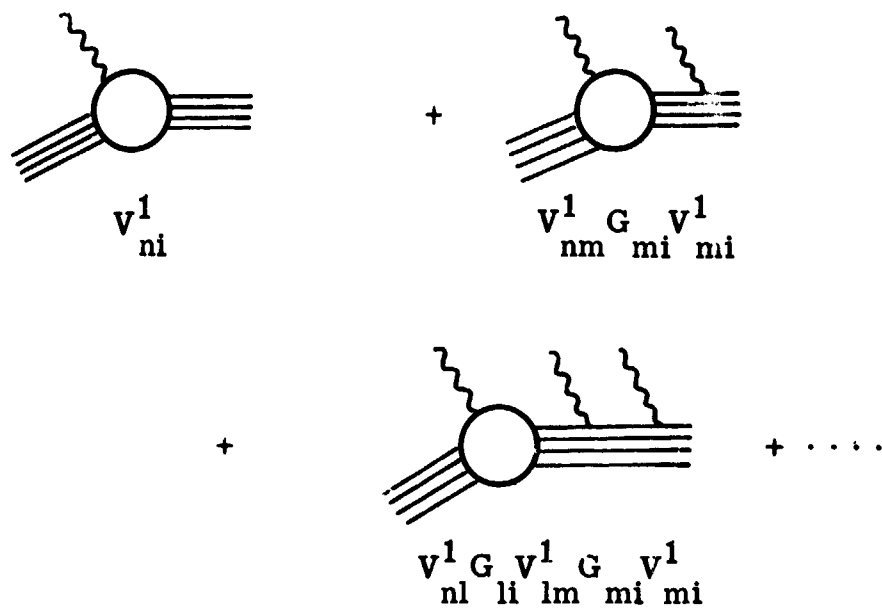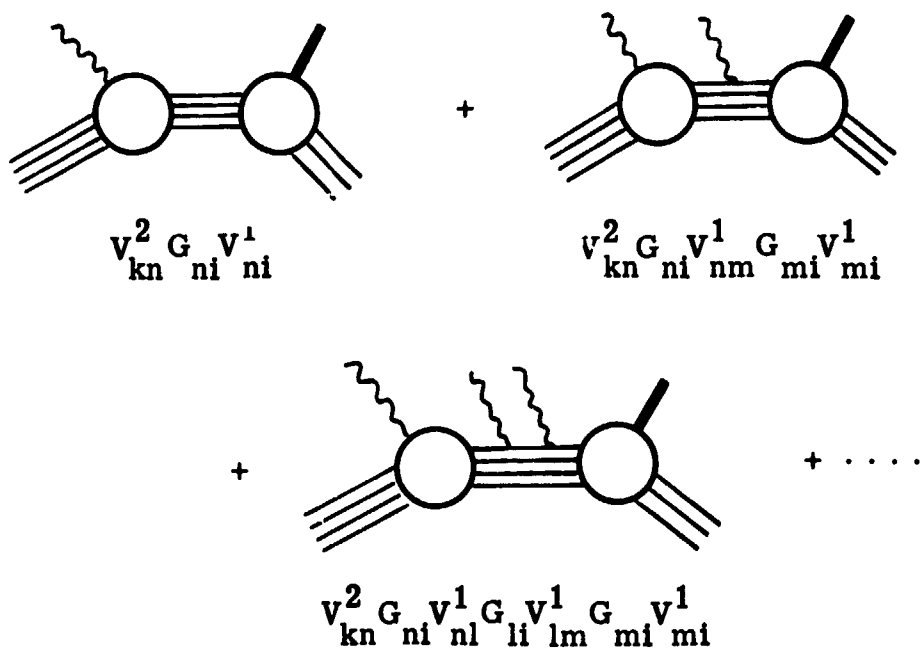
Figure 11. Abrasion to all orders.

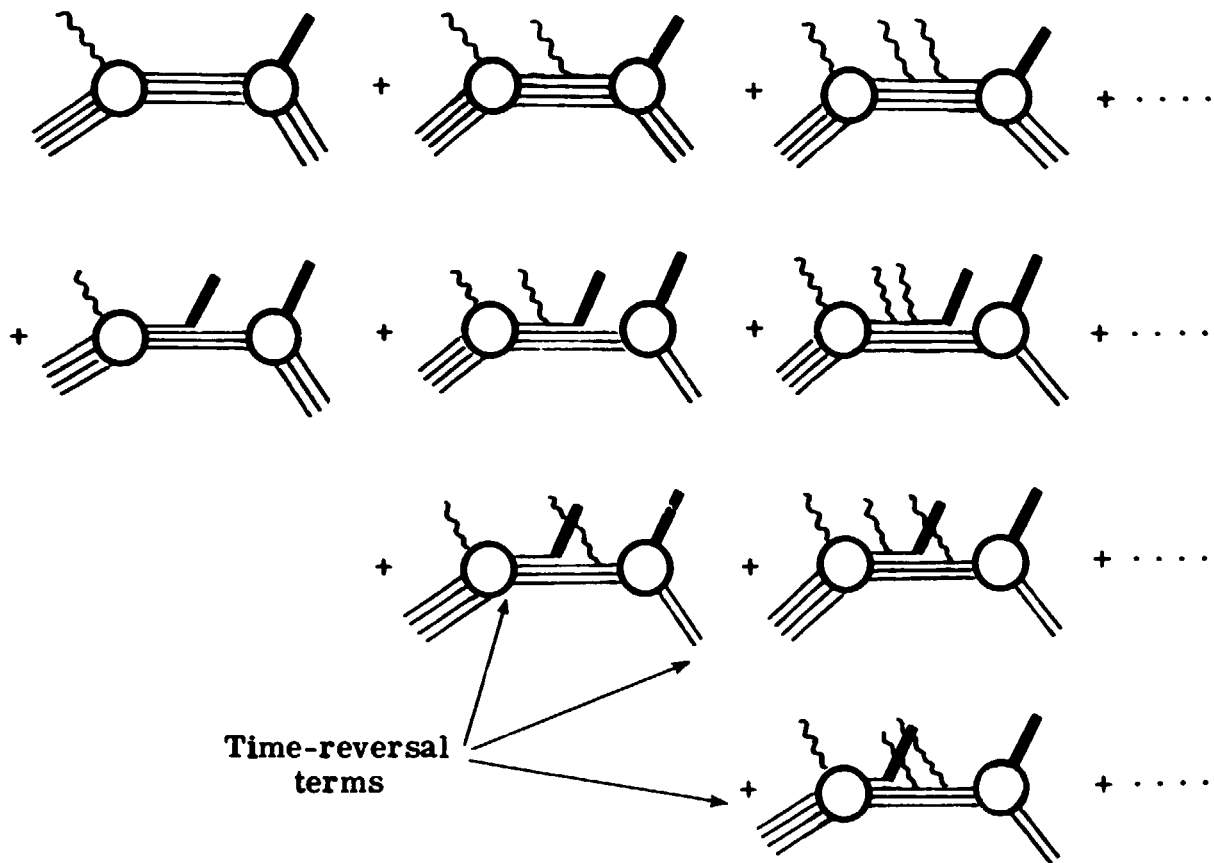Figure 12. Abrasion to all orders with ablation to first order.

Figure 13. Abrasion to all orders with Ablation to second order.